Single crystals of $RAlO_3$ (R: Dy, Ho and Er) for use in magnetic refrigeration between 4.2 and 20 K

H. KIMURA, T. NUMAZAWA, M. SATO
National Research Institute for Metals, 1-2-1 Sengen, Tsukuba, Ibaraki 305, Japan
T. IKEYA*, T. FUKUDA
Institute for Materials Research, Tohoku University, 2-1-1 Katahira, Aoba-ku, Sendai 980-77, Japan
K. FUJIOKA
Daido Hoxan Inc., 3-16-2 Ninomiya, Tsukuba, Ibaraki 305, Japan

Single crystals of $RAlO_3$ (R: Dy, Ho and Er) were grown using the Czochralski technique. The magnetization of the single crystals along the *a*-, *b*- and *c*-axes was measured in the paramagnetic region using a superconducting quantum interference device (SQUID) magnetometer. Using these values of the magnetization, the magnetic entropy change, which depends on the crystal axis direction, was calculated. Single crystals of $DyAlO_3$ oriented along the *b*-axis and *c*-axis oriented $ErAlO_3$ single crystals are promising materials for use in magnetic refrigeration systems using the Carnot cycle in the temperature range between 4.2 and 20 K.

1. Introduction
Magnetic refrigeration, which utilizes the properties of the paramagnetic phase of antiferromagnetic materials by the application of a magnetic field, has been proposed as a new refrigeration system to produce liquid helium (at 4.2 K) or superfluid helium (at 1.8 K) with a higher efficiency than that of normal gas refrigeration [1]. The Carnot cycle, which consists of adiabatic and isothermal processes, has been applied in magnetic refrigeration because it is easy to set up and effective at temperatures below 20 K. Magnetic materials for application in magnetic refrigeration (magnetic refrigerants) using the Carnot cycle have to possess the following characteristics; (1) a large magnetic entropy change (magneto-thermal property), (2) an optimum magnetic phase-transition temperature (from antiferromagnetic to paramagnetic behavior), (3) a small heat capacity and (4) a large thermal conductivity when an electronic insulator.

Rare-earth garnet single crystals, such as $Gd_3Ga_5O_{12}$ and $Dy_3Al_5O_{12}$ that have a cubic symmetry, have been applied in magnetic refrigeration [2] because of their large magnetic entropy change; a large thermal conductivity and the facile growth of large high quality single crystals of these materials. Perovskite structured orthoaluminate single crystals of the type $RAlO_3$ (R: Gd, Dy and Er) have been suggested, on the basis of a theoretical study [3], to be potentially more efficient magnetic refrigerants in the temperature range of interest. The magneto-thermal properties of $RAlO_3$ (R: Dy, Ho and Er) along the *c*-axis of the orthorhombic unit cell has been reported in the literature [4] to possess a large effective Bohr magneton number (Dy: 10.63, Ho: 10.60 and Er: 9.59 $\mu_B = 9.214 \times 10^{-24}\ J \cdot T^{-1}$). It should be noted that single crystal growth of $GdAlO_3$ is very difficult due to its melting temperature $> 2000\,^{\circ}C$ [4]. Since the orthoaluminate systems crystallize into orthorhombic symmetry phases ($a \neq b \neq c$), see Table I, it follows that there will be anisotropic behaviour in the properties of these systems. It is therefore important to investigate the dependence of the paramagnetic behaviour on crystalline orientation in the temperature range between the magnetic phase transition temperature down to 20 K.

In the present work, we focus on the anisotropic magneto-thermal properties of single crystal $RAlO_3$ (R: Dy, Ho and Er) and evaluate the dependence of the paramagnetic properties on the crystal axis direction on the basis of magnetization studies. In addition the thermal conductivity is measured along the *c*-axis growth direction. Finally the potential of $RAlO_3$ as an magnetic refrigerant is evaluated.

2. Experimental procedures
Single crystals of $RAlO_3$ (R: Dy, Ho and Er) were grown by the Czochralski method using an iridium

* *Present address*: Fujitsu Laboratories Ltd., 64 Nishiwaki-Okubocho, Akashi, Hyogo 674, Japan.

0022–2461

TABLE I Lattice parameters of $RAlO_3$ in nm [5]

$RAlO_3$	Axis	*a*	*b*	*c*
$DyAlO_3$		0.5207	0.5318	0.7396
$HoAlO_3$		0.5181	0.5323	0.7374
$ErAlO_3$		0.5162	0.5326	0.7359

crucible 50 mm in diameter and 50 mm in height in an RF coil [6]. The starting materials were; R_2O_3 (R: Dy, Ho and Er) and Al_2O_3 powders with a 99.99% purity. The oxide powders were heated prior to mixing in order to eliminate absorbed moisture and gases. Then they were weighed, mixed, pressed and sintered at 1200 °C for 24 h in an air atmosphere. The presence of the perovskite structured phase was confirmed by powder X-ray diffraction analysis. All crystals were grown in an Ar atmosphere. The pulling rate was $5\ \mathrm{mm\,h^{-1}}$ and the rotation rate was either 5 or 20 r.p.m. A single crystal of $YAlO_3$ was used as the seed crystal because of its similar lattice parameter and melting temperature. The growth direction was the *c*-axis ([001]) which was the easiest direction to grow; therefore it is probable that only crystals grown in this direction have any chance of finding application as a magnetic refrigerant.

Samples, for the magnetization measurements, were prepared from the grown single crystals with great care being exercised to avoid any sections that contained crystallographic twins. The measurement sample had a rectangular shape of $1 \times 1 \times 8$ mm with each of the *a*-, *b*- and *c*-axes becoming the long axis in a sample. The magnetization measurements were performed over the temperature range of 4.2–20 K in applied magnetic fields up to 50 kOe (1 Oe = $79.58\ \mathrm{Am^{-1}}$) superconducting quantum interference device (SQUID) magnetometer to apply the magnetic field parallel to each axis. The demagnetization factor was evaluated to be less than 0.02 and thus it could be ignored. The magnetic susceptibility was extracted from magnetization measurement performed in a weak applied magnetic field below 10 kOe.

The thermal conductivity was measured by a steady state method using a sample of size $6 \times 6 \times 40$ mm along *c*-axis in the temperature range of 4.2–20 K.

3. Results and discussion

Fig. 1(a–c) show a grown single crystal of $DyAlO_3$, $HoAlO_3$ and $ErAlO_3$ respectively. The grown crystals were transparent and were 10–20 mm in diameter and 20–50 mm in length having a colour (yellow, brown and purple) induced by the rare earth 4f electrons. Fig. 2(a–c) shows the image under crossed polarizers of wafers cut perpendicular to the *c*-axis. Multiple twins were observed in $DyAlO_3$, with fewer twins being observed in the $HoAlO_3$ and $ErAlO_3$ samples. These results imply the difficulty of growing large single crystals of $DyAlO_3$. That is to say, the temperature gradient is small at the solid–liquid interface during the crystal growth due to a large optical absorption in single crystal $DyAlO_3$ [6]. All twins were

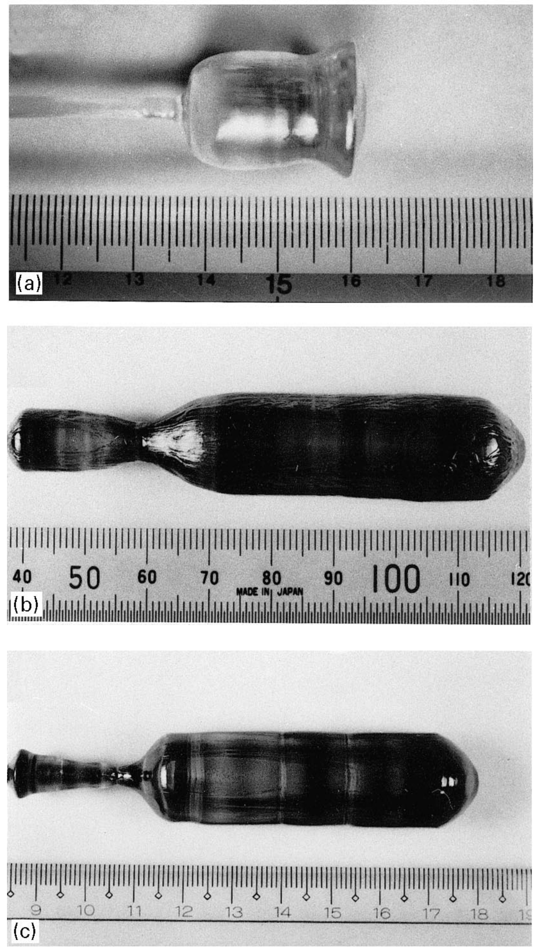

Figure 1 Single crystals 10–20 mm in diameter and 20–50 mm in length. (a) $DyAlO_3$, (b) $HoAlO_3$ and (c) $ErAlO_3$.

observed to exist along the *c*-axis, so that the effect on the thermal conductivity, which is an important property for application as a magnetic refrigerant, was presumed to be small.

Fig. 3(a–c) shows the temperature dependence of the magnetization along each axis. In these samples the *a*-axis lattice parameter is close to that of the *b*-axis with a significantly different *c*-axis being observed [5]. The magnetization was almost constant along the *c*-axis in $HoAlO_3$ and $DyAlO_3$ with a small maximum peak being observed near 12 K in $HoAlO_3$. On the other hand, the magnetization rapidly decreased with increasing temperature along the other axes in the other single crystals.

Fig. 4(a–c) shows the temperature dependence of the inverse magnetic susceptibility. The values closely follow the Curie–Weiss law over the whole temperature range measured above the magnetic phase-transition temperature (Néel temperature) which for the *c*-axis has been reported to be 3.5 K in $DyAlO_3$ [7] and 0.6 K in $ErAlO_3$ [8], whilst no value is available for $HoAlO_3$. We think that the result for $HoAlO_3$ is due to crystal field effects but no detailed understanding of this problem is currently available. The paramagnetic Curie temperature over the investigated temperature range was estimated to be negative, so that $RAlO_3$ (R: Dy, Ho and Er) would possess antiferromagnetic properties below the magnetic phase-transition temperature.

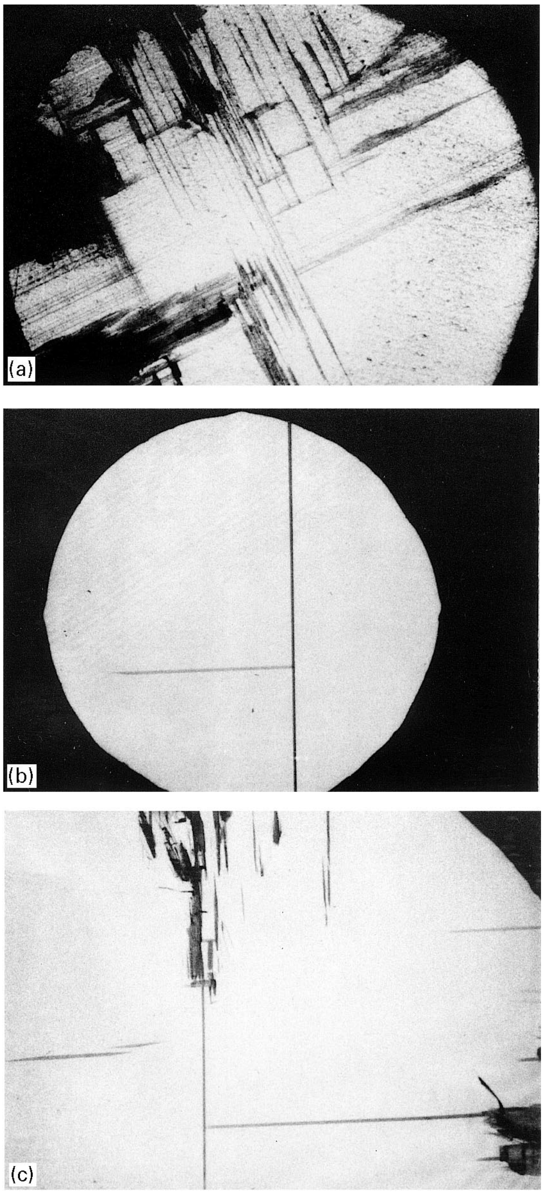

Figure 2 Image under crossed polarizers of wafers cut perpendicular to the c-axis. (a) $DyAlO_3$, (b) $HoAlO_3$ and (c) $ErAlO_3$.

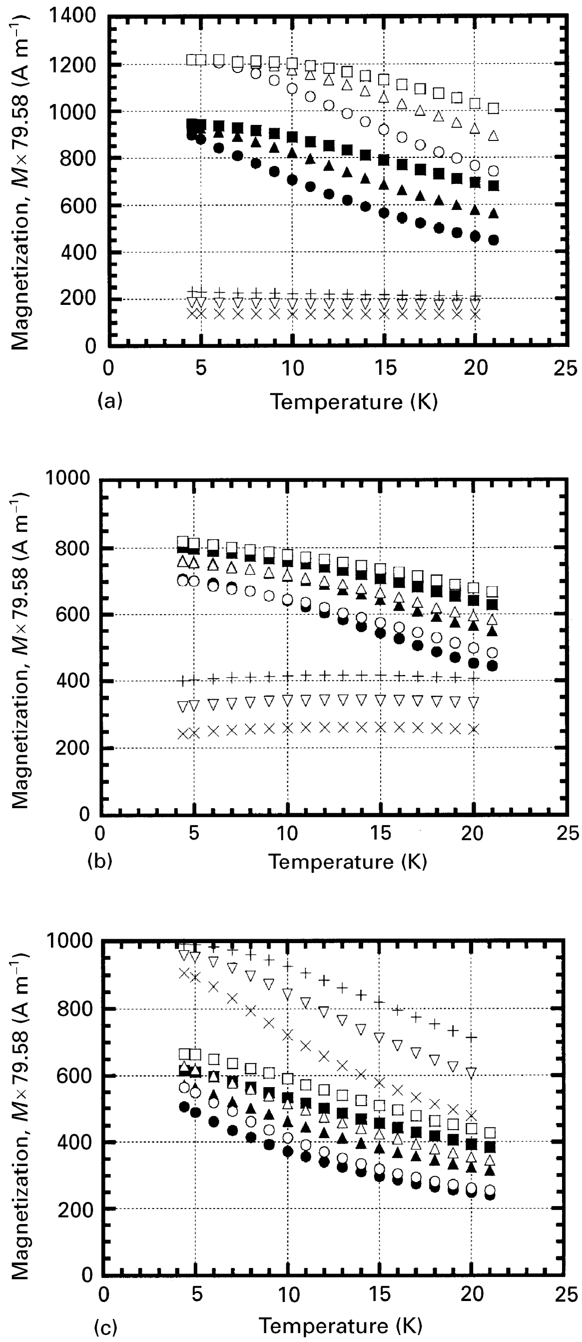

Figure 3 Temperature dependence of the magnetization, M, along the a- (●, ▲, ■), b- (○, △, □) and c-axes (×, ▽, +) at applied magnetic fields of 30, 40 and 50 kOe (1 Oe = 79.58 Am^{-1}) respectively. (a) $DyAlO_3$, (b) $HoAlO_3$ and (c) $ErAlO_3$.

Fig. 5(a–c) shows the temperature dependence of the magnetic entropy change, ΔS_M, calculated from the results presented in Fig. 3(a–c) [9]. A negative value means a decrease in the ΔS_M value. The absolute values of ΔS_M generally decreased with an increase in the temperature. The behaviour of ΔS_M along the b-axis in $DyAlO_3$ and along the c-axis in $ErAlO_3$ are in agreement with the theoretical calculations of Kuz'min and Tishin [3]. Large anisotropic magnetothermal properties are observed for all the $RAlO_3$ (R: Dy, Ho and Er). In $HoAlO_3$, curious results were obtained along the c-axis reflecting the temperature dependence of the magnetization in Fig. 3b.

Fig. 6 is a comparison of the temperature dependence of ΔS_M along the $DyAlO_3$ b-axis and the $ErAlO_3$ c-axis, together with those along the $\langle 1\,1\,1 \rangle$ direction in $Dy_3Al_5O_{12}$ and $Gd_3Ga_5O_{12}$ [10]. The ΔS_M values in $DyAlO_3$ and $ErAlO_3$ are superior to those in $Dy_3Al_5O_{12}$ and $Gd_3Ga_5O_{12}$ in the temperature range of 4.2–20 K. Since the ΔS_M value for $DyAlO_3$ is large up to 20 K, this material will be a more effective magnetic refrigerant than $ErAlO_3$.

Fig. 7 shows the thermal conductivity, λ, along the c-axes of the $DyAlO_3$, $HoAlO_3$ and $ErAlO_3$ single crystals, together with those along the $\langle 1\,1\,1 \rangle$ direction of $Dy_3Al_5O_{12}$ and $Gd_3Ga_5O_{12}$ single crystals. A λ value above 1 $WK^{-1}\,cm^{-1}$ is required for a material to be of interest for use in a magnetic refrigeration system. The λ values for all the investigated orthoaluminate single crystals are larger than that in $Dy_3Al_5O_{12}$, which is already used in magnetic refrigeration systems [2]. No significant effects due to the existence of the twins in the $DyAlO_3$ crystals was observed.

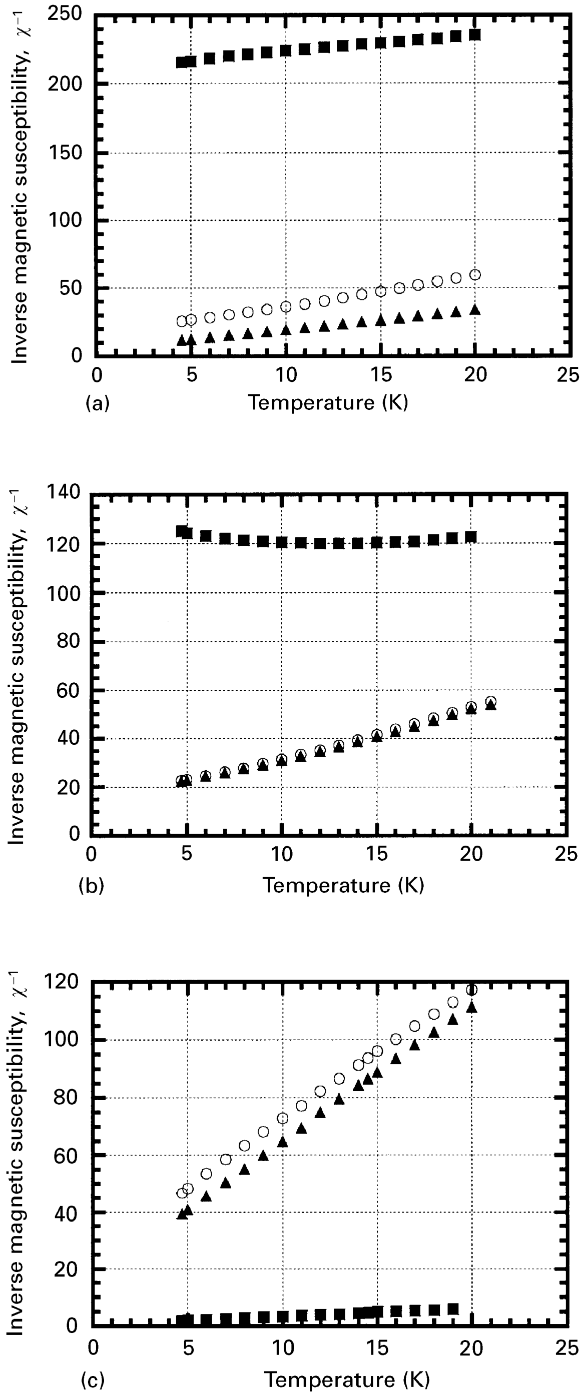

Figure 4 Temperature dependence of the inverse magnetic susceptibility, χ^{-1}. (a) $DyAlO_3$, (b) $HoAlO_3$ and (c) $ErAlO_3$. (○), *b*- (▲) and *c*-axes (■).

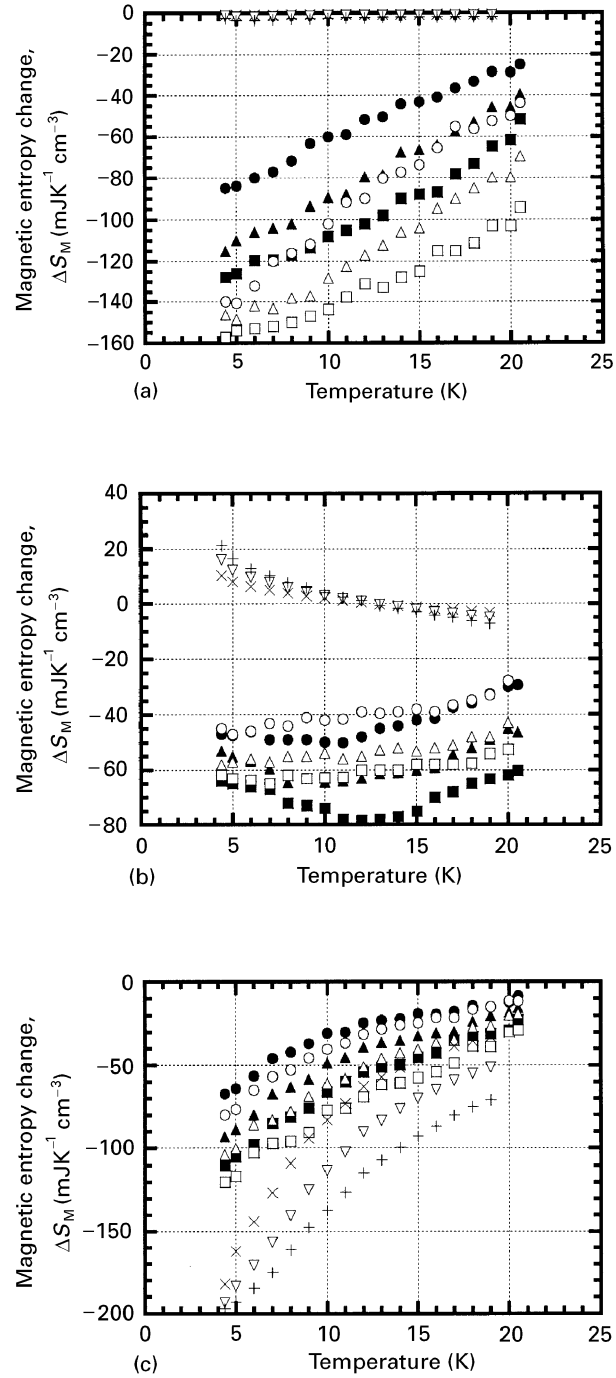

Figure 5 Temperature dependence of the magnetic entropy change, ΔS_M, along *a*- (●, ▲, ■), b- (○, △, □) and *c*-axes (×, ▽, +) at applied magnetic fields of 30, 40 and 50 kOe (1 Oe = 79.58 Am^{-1}) respectively. (a) $DyAlO_3$, (b) $HoAlO_3$ and (c) $ErAlO_3$.

On the basis of the ΔS_M, values *b*-axis oriented $DyAlO_3$ and *c*-axis oriented $ErAlO_3$ single crystals have potential as magnetic refrigerants at temperatures below 20 K. The $DyAlO_3$ and $ErAlO_3$ single crystals have large thermal conductivities, comparable to those of single crystals of $Dy_3Al_5O_{12}$ and $Gd_3Ga_5O_{12}$ in the temperature range below 20 K [11]. However, for practical uses, it is difficult to grow large size single crystals of $DyAlO_3$ even along the *c*-axis. Single crystal $ErAlO_3$ which can be grown along the *c*-axis is a practical magnetic refrigerant.

4. Conclusion

The magnetization values of single crystals of $RAlO_3$ (R: Dy, Ho and Er) have been measured using a SQUID magnetometer. From the viewpoint of application as a magnetic refrigerant *b*-axis oriented single crystals of $DyAlO_3$ and *c*-axis oriented $ErAlO_3$ single crystals are promising candidate materials for inclusion in refrigerators to produce liquid helium (4.2 K) in the temperature range below 20 K. Single crystals of $ErAlO_3$ are easy to grow whereas those $DyAlO_3$ are difficult to grow and further study of its growth is required.

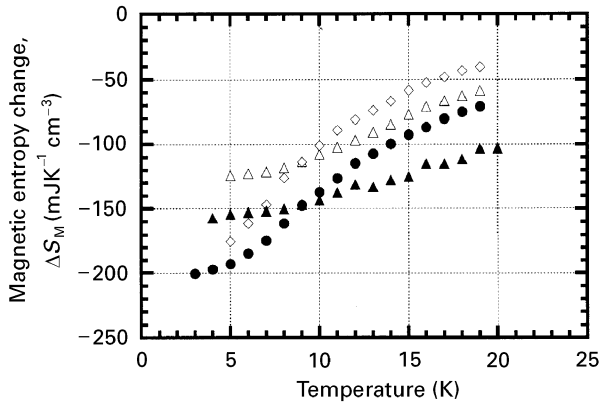

Figure 6 Comparison of temperature dependence of magnetic entropy change, ΔS_M, in $DyAlO_3$ (▲) along the *b*-axis and in $ErAlO_3$ (●) along the *c*-axis, together with those in $Dy_3Al_5O_{12}$ (△) and $Gd_3Ga_5O_{12}$ (◇) along ⟨1 1 1⟩ direction, at applied magnetic field of 50 kOe (1 Oe = 79.58 Am^{-1}).

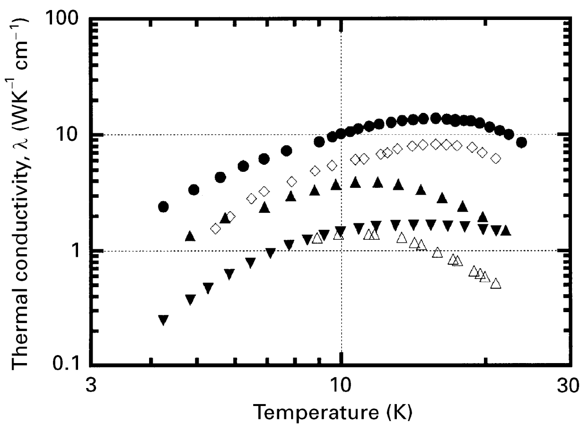

Figure 7 Temperature dependence of thermal conductivity, λ, for single crystals of $DyAlO_3$ (▲), $HoAlO_3$ (▼) and $ErAlO_3$ (●) along the *c*-axis, together with those in $Dy_3Al_5O_{12}$ (△) and $Gd_3Ga_5O_{12}$ (◇) along the ⟨1 1 1⟩ direction.

Acknowledgements

Part of this work was performed under the Visiting Researcher's Program of the Laboratory for Development Research of Advanced Materials, Institute for Materials Research, Tohoku University.

References

1. A. F. LACAZE, R. BERANGER, G. BON MARDION, G. CLAUDET and A. A. LACAZE, *Cryogenics* **23** (1983) 427.
2. T. NUMAZAWA, H. KIMURA, M. SATO and H. MAEDA, *ibid.* **33** (1993) 547.
3. M. D. KUZ'MIN and A. M. TISHIN, *J. Phys. D: Appl. Phys.* **24** (1991) 2039.
4. H. KIMURA, T. NUMAZAWA, M. SATO, T. IKEYA and T. FUKUDA, *J. Appl. Phys.* **77** (1995) 432.
5. JCPDS cards. $DyAlO_3$ (39-1437), $HoAlO_3$ (24-470) and $ErAlO_3$ (24-396).
6. Y. OKANO, T. IKEYA, K. HOSHIKAWA and T. FUKUDA, *J. Cryst. Growth* **131** (1993) 616.
7. H. SCHUCHERT, S. HUFNER and R. FAULHABER, *Z. Physik* **222** (1969) 105.
8. J. SIVARDIERE and S. QUUEZEL-AMBRUNAZ, *C.R. Acad. Sci. Paris* **273** (1971) 619.
9. T. HASHIMOTO, T. NUMAZAWA, M. SHINO and T. OKADA, *Cryogenics* **21** (1981) 647.
10. R. LI, T. NUMAZAWA, T. HASHIMOTO, A. TOMOKIYO, T. GOTO and S. TODO, *Advan. Cryo. Engng. Mater.* **32** (1986) 287.
11. T. NUMAZAWA, H. KIMURA, M. SATO, T. IKEYA, K. SHIMAMURA and T. FUKUDA, *J. Mater. Sci.* (in press).

Received 7 May 1996
and accepted 28 April 1997